Magnetorotational instability: a review

Shi Sim, David P. Larson, and Wonjae Lee

University of California, San Diego

(Received 3 June 2013)

We review current research on magneotorotational instability (MRI) as a mechanism for momentum transporation in accretion disks.

1. Introduction

Turbulence generating magnetorotational Instability (MRI) was first discovered by Velikhov (1959) and Chandrasekhar (1960) and was later re-discovered by Balbus and Hawley (1998) for astrophysical applications. MRi has since then been confirmed by robust numerical simulations although not experimentally or through observations. To understand the importance of MRI, we have to look into the accretion disk theory where many astrophysical phenomena take place in.

Accretion disks are disk made up of gas, dust, and plasma that rotates around and gradually collapses onto an object in the center, e.g leading to formation of a star. However, accretion can happen only with an efficient mechanism for rapidly transporting angular momemtum outwards. It was suggested that turbulence drives angular momentum outwards but there was no known mechanism that would generate turbulence. These Keplerian disks satisfies the Rayleigh stability criterion (Rayleigh 1916) against centrifugal instability. Thus, there has to be other mechanisms that generates turbulence and this is where MRI and non-linear hydrodynamic instablities comes into the picture. There has been other mechanisms suggested but MRI seem like the most probable explanation at this point.

MRI is not only applicable to astrophysical phenomena but geophysical ones as well, e.g Earth's magnetic field. It is used to better understand how planetary magnetic field might have formed on Earth or other planets and how and why the field is sustained or decayed through time.

In this report, we attempt to explain and illustrate the instability in an astrophysical sense and go through what has been done experimentally and numerically in terms of MRI.

2. Physical Explanation

2.1. *Perfectly conducting fluid in magnetic field*

The magnetic field lines are tied to the conducting fluid in which they are embedded. We can show this by comparing a transport equation of magnetic field with a equation for a line element moving with fluid. We first combine Ohm's Law in ideal conductor and Faraday's equation to get a transport equation for magnetic field,

$$\begin{aligned}\frac{\partial \mathbf{B}}{\partial t} &= \nabla \times (\mathbf{u} \times \mathbf{B}) \\ &= \mathbf{B} \cdot \nabla \mathbf{u} - \mathbf{u} \cdot \nabla \mathbf{B} - \mathbf{B} \nabla \cdot \mathbf{u}. \end{aligned} \tag{2.1}$$

Assuming incompressibility, we get,

$$\frac{D\mathbf{B}}{Dt} = (\mathbf{B}\cdot\nabla)\mathbf{u}, \tag{2.2}$$

where $\frac{D}{Dt}$ is the convective derivative $\frac{D}{Dt} = \frac{\partial}{\partial t} + (\mathbf{u}\cdot\nabla)$.

Considering a short line element $d\mathbf{l}$ moving with fluid, we can express the rate of change of $d\mathbf{l}$ as

$$\frac{D}{Dt}(d\mathbf{l}) = \mathbf{u}(\mathbf{x}+d\mathbf{l}) - \mathbf{u}(\mathbf{x}) = (d\mathbf{l}\cdot\nabla)\mathbf{u}. \tag{2.3}$$

Comparing two equations above, we can conclude that $\mathbf{B}$ and $d\mathbf{l}$ obey the same equation (see Davidson 2001). Therefore, the field lines are frozen into the fluid.

2.2. *Magnetic tension*

When the fluid elements are displaced from their equilibrium position, the magnetic field lines move together with fluid elements and behave like elastic bands frozen-into the fluid. Using Ampere's law, the Lorenz force ($\mathbf{J}\times\mathbf{B}$) may be written as

$$\mathbf{J}\times\mathbf{B} = -\nabla\left(\frac{B^2}{2\mu}\right) + \frac{(\mathbf{B}\cdot\nabla)\mathbf{B}}{\mu} = -\nabla\left(\frac{B^2}{2\mu}\right) + \frac{\partial}{\partial s}\left[\frac{B^2}{2\mu}\right]\hat{e}_t - \frac{B^2}{\mu R}\hat{e}_n \tag{2.4}$$

where R is radius of curvature and s is a coordinate along a magnetic field line. $\hat{e}_t$ and $\hat{e}_n$ are tangential and normal unit vectors respectively. The last two terms are magnetic tension forces in tangential and normal directions. These forces can also be interpreted as tensile stress of $B^2/2\mu$ acting on the end of the tube (see Davidson 2001).

This tensile force which is also know as Faraday or Maxwell tension is analogous to a force acting on a spring. Considering a displacement $\boldsymbol{\xi} = \mathbf{v}\delta t$, the Faraday's equation can be written as $\delta\mathbf{B} = ikB\boldsymbol{\xi}$. The magnetic tension for small displacement per unit density ρ is

$$\frac{(\mathbf{B}\cdot\nabla)\delta\mathbf{B}}{\mu\rho} = \frac{ikB\delta\mathbf{B}}{\mu\rho} = -\frac{k^2B^2}{\mu\rho}\boldsymbol{\xi} = -K\boldsymbol{\xi}, \tag{2.5}$$

where K is comparable to the spring constant (see Wikipedia 2013; Balbus & Hawley 1998). The equation has same form of Hooke's Law for a spring.

2.3. *Magnetoroational instability*

Consider Keplerian motion of conducting fluid orbiting around a central body of mass M_c. Two adjacent fluid elements m_i and m_o at radial position r_i and r_o are orbiting around gravitational center with angular velocity $\Omega_i = \sqrt{\frac{GM_c}{r_i^3}}$ and $\Omega_o = \sqrt{\frac{GM_c}{r_o^3}}$ respectively. Therefore the angular velocity of the inner element is higher than that of the outer elements $\left(\frac{d\Omega^2}{dr} < 0\right)$, but the angular momentum of the inner element is smaller than that of the outer element $\left(\frac{dr^4\Omega^2}{dr} > 0\right)$.

If a magnetic field line is connecting the conducting fluid elements, the magnetic field will move together with the two elements. Because of the velocity shear in Keplerian motion, the magnetic field will be stretched and bent. Therefore the magnetic field will exert restoring force on the fluid element making the inner element pulled back and the outer element dragged forward. The inner element lose angular momentum, therefore it must fall to an orbit of smaller radius. On the other hand the outer element gains angular momentum and moves to the orbit of larger radius. This outward angular momentum transport makes the small initial displacement get larger. The

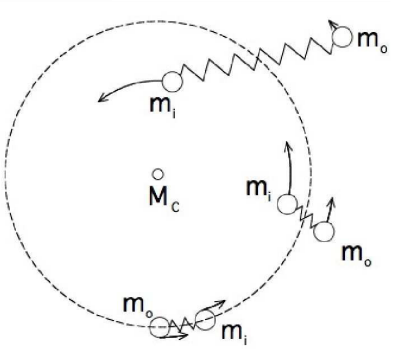

[t]

FIGURE 1. A schematic diagram from Balbus (2009) showing magnetorotational instability. Two fluid elements m_i (inner) and m_o (outer) orbit a mass (M_C) with the magnetic tension between the two elements represented by a spring. Over time m_i loses angular momentum, moving closer to M_C while m_o gains angular momentum and moves away from M_C.

magnetic fields are stretched even more and gives positive feedback leading the system unstable. This instability is known as a magnetorotational instability (MRI) and is illustrated in Figure 1.

One can show that the dispersion relation for the incompressible ideal flow rotating with angular velocity Ω_0 is

$$\omega^4 - \left[2\left(k^2V_A^2\right) + \kappa^2\right]\omega^2 + \left(k^2V_A^2\right)\left[\left(k^2V_A^2\right) + r\frac{d\Omega^2}{dr}\right] = 0, \tag{2.6}$$

where ω and k are angular frequency and wave number of a perturbation $\xi \propto e^{i(kz+\omega t)}$. $V_A = \frac{B}{\sqrt{\mu\rho}}$ is Alfvén speed for the imposed magnetic field B. κ^2 is known as epicylic frequency $\left(\kappa^2 = 4\Omega_0^2 + r\frac{d\Omega^2}{dr}\right)$ (see Balbus & Hawley 1991; Balbus & Hawley 1998; Balbus 2003). If $\frac{d\Omega^2}{dr} < 0$, then one of ω^2 has negative root for long wave length modes satisfying

$$k^2 < -\frac{r}{V_A^2}\frac{d\Omega^2}{dr}. \tag{2.7}$$

Therefore, the instability criterion for the magnetorotational instability (MRI) is represented as radially decreasing angular velocity,

$$\frac{d\Omega^2}{dr} < 0 \quad \text{(UNSTABLE)} \tag{2.8}$$

Note that the MRI is different from the conventional hydrodynamic instability known as Couette-Taylor centrifugal instability (see Charru & de Forcrand-Millard 2011). The Couette-Taylor centrifugal instability criterion for axsymmetric perturbation is represented as radially decreasing angular momentum,

$$\frac{dr^4\Omega^2}{dr} < 0 \quad \text{(UNSTABLE)} \tag{2.9}$$

The Keplerian disk is a good example of flows which are stable to the hydrodynamic instability but unstable to the MRI.

3. Theoretical Work

Acheson & Hide (1973) and Knobloch (1992) showed the linear stability analysis of rotating magneto-fluid bounded in coaxial cylinder. For the case of gaseous astrophysical disks in unbounded geometry was shown in Balbus & Hawley (1991). The condition for stability was shown to be radially increasing angular velocity profile. We present a linear stability analysis of MRI for radially bounded case following Acheson (1972), Acheson (1973), Knobloch (1992), and Julien & Knobloch (2010).

3.1. *Governing equation*

The wave dispersion equation of a cylindrical magneto-fluid can be obtained from the magnetohydrodynamic (MHD) equations. Assuming the fluid is inviscid and perfectly conducting, the ideal MHD equations are

$$\rho\left(\frac{\partial \mathbf{u}}{\partial t}+\mathbf{u}\cdot\nabla\mathbf{u}\right)=-\nabla p+\mathbf{J}\times\mathbf{B} \tag{3.1}$$

$$\frac{\partial \rho}{\partial t}+\nabla\cdot(\rho\mathbf{u})=0 \tag{3.2}$$

$$\frac{d}{dt}\left(\frac{p}{\rho^{\gamma}}\right)=0 \tag{3.3}$$

$$\mathbf{E}+\mathbf{u}\times\mathbf{B}=0 \tag{3.4}$$

$$\nabla\times\mathbf{E}=-\frac{\partial \mathbf{B}}{\partial t} \tag{3.5}$$

$$\nabla\times\mathbf{B}=\mu\mathbf{J}, \tag{3.6}$$

where $\mathbf{u}$ fluid velocity, ρ is fluid denstity, p is pressure. $d/dt=\partial/\partial t+\mathbf{u}\cdot\nabla$ is convective derivative and γ is the ratio of specific heats. $\mathbf{E}$, $\mathbf{B}$ and $\mathbf{J}$ are electic field, magnetic field and current density respectively (see Freidberg 1987).

To investigate the magnetorotational instability, one can consider homogeneous incompressible fluid rotating with angular velocity $\Omega(r)=\frac{V(r)}{r}$ in externally imposed magnetic fields $\mathbf{B}_0=[0,B_\phi(r),B_z(r)]$. Combining electromagnetic equations with momentum relation, we get the appropriate MHD equations,

$$\frac{\partial \mathbf{u}}{\partial t}+(\mathbf{u}\cdot\nabla)\mathbf{u}=-\frac{1}{\rho}\nabla\left(P+\frac{\mathbf{B}^2}{2\mu}\right)+\frac{1}{\mu\rho}(\mathbf{B}\cdot\nabla)\mathbf{B} \tag{3.7}$$

$$\frac{\partial \mathbf{B}}{\partial t}+(\mathbf{u}\cdot\nabla)\mathbf{B}=(\mathbf{B}\cdot\nabla)\mathbf{u} \tag{3.8}$$

$$\nabla\cdot\mathbf{u}=0 \tag{3.9}$$

$$\nabla\cdot\mathbf{B}=0. \tag{3.10}$$

3.2. *Linear perturbation equation and eigenvalue problem*

We can get linearized equations by perturbing the basic state by small amount of $\mathbf{u_1}$ and $\mathbf{b_1}$ for velocity and magnetic fields. The linear perturbation is assumed to have the form

$$f=\Re\left[\hat{f}(r)e^{i(m\phi+kz+\omega t)}\right]. \tag{3.11}$$

Accoring to Acheson (1972), the normal mode equations are

$$\hat{b}_r = \frac{\hat{u}_r}{\omega}\left(kB_z + \frac{mB_\phi}{r}\right), \tag{3.12}$$

$$\hat{b}_\phi = -\frac{(\hat{u}_r B_\phi)'}{i\omega} + \frac{k}{\omega}(\hat{u}_\phi B_z - \hat{u_z} B_\phi), \tag{3.13}$$

$$\hat{b}_z = -\frac{(r\hat{u}_r B_z)'}{ri\omega} - \frac{m(\hat{u_\phi} B_z - \hat{u}_z B_\phi)}{r\omega}, \tag{3.14}$$

$$\hat{u}_z = -\frac{(r\hat{u}_r)'}{rik} - \frac{m\hat{u}_\phi}{rk}, \tag{3.15}$$

$$\left(1 + \frac{m^2}{r^2k^2}\right) ri\hat{u}_\phi = -\frac{m}{rk^2}(r\hat{u}_r)' - \frac{\hat{u}_r}{\left(V_{Az} + \frac{mV_{A\phi}}{rk}\right)^2 \frac{k^2}{\omega^2} - 1}\left\{-\frac{2\Omega r}{\omega} + \frac{2kV_{A\phi}}{\omega^2}\left(V_{Az} + \frac{mV_{A\phi}}{rk}\right)\right\}, \tag{3.16}$$

where $V_{A\phi} = \frac{B_\phi(r)}{\sqrt{\mu\rho}}$, $V_{Az} = \frac{B_z(r)}{\sqrt{\mu\rho}}$ are Alfvén speeds for associated external magnetic field components.

Solving the normal mode equation set for radial velocity perturbation $\hat{u}_r = u$ and considering axisymmetric perturbation ($m = 0$), Acheson (1973) obtained following eigenvalue problem,

$$\frac{d}{dr}\left[(\omega^2 - k^2V_{Az}^2)\left(\frac{du}{dr} + \frac{u}{r}\right)\right] - k^2\left[\omega^2 - k^2V_{Az}^2 + r\frac{d}{dr}\left(\frac{V_{A\phi}^2}{r^2} - \frac{V^2}{r^2}\right)\right]u = -\frac{4k^2}{r^2}\frac{(kV_{A\phi}V_{Az} + \omega V)^2}{(\omega^2 - k^2V_{Az}^2)}u. \tag{3.17}$$

3.3. *Stability criterion*

3.3.1. *Standard magnetorotational instability*

Consider a standard MRI of radially bounded coaxial fluid cylinder with externally imposed axial magnetic field but without axial current flowing. Therefore, we have $V_{Az} = \frac{B_z}{\sqrt{\rho\mu}} = const \neq 0$ and $V_{A\phi} = \frac{B_\phi}{\sqrt{\rho\mu}} = 0$. Considering boundary condition $u(r_1) = u(r_2) = 0$, we multiply the eigenvalue equation by complex conjugate of u and integrate over radial coordinate,

$$(\omega^2 - k^2V_{Az}^2)^2 = \frac{k^2}{D}\int_{r_1}^{r_2}\left[\frac{\omega^2}{r^2}\frac{d}{dr}r^2V^2 - r^2k^2V_{Az}^2\frac{d}{dr}\left(\frac{V^2}{r^2}\right)\right]|u|^2dr \tag{3.18}$$

where

$$D \equiv \int_{r_1}^{r_2}\left(r\left|\frac{du}{dr}\right|^2 + \frac{|u|^2}{r} + k^2r|u|^2\right)dr > 0 \tag{3.19}$$

Accoring to Chandrasekhar (1960), ω^2 must be real. We get stable modes with $\omega^2 > 0$ and unstable modes with $\omega^2 < 0$. If the angular velocity increases radially outward, $\frac{d}{dr}\left(\frac{V^2}{r^2}\right) > 0$, the

system is stable because ω^2 is bounded from below by positive number,

$$\omega^2 > \frac{r^2 k^2 V_{Az}^2 \frac{d}{dr}\left(\frac{V^2}{r^2}\right)}{4\frac{V^2}{r} + r^2 \frac{d}{dr}\left(\frac{V^2}{r^2}\right)} > 0. \tag{3.20}$$

If we have radially decreasing anguar velocity profile, $\frac{d}{dr}\left(\frac{V^2}{r^2}\right) < 0$, somewhere $r_1 < r < r_2$, then ω^2 may have negative solution which makes the system unstable.

3.3.2. *Helical magnetorotational instability*

When the external nonzero magnetic fields in axial and azimuthal directions are considered, it was found that the eigenvalue equation can be written as

$$\frac{d}{dr}r\frac{du}{dr} - \frac{u}{r} - k^2 ru = \frac{k^2}{(\omega^2 - k^2 V_{Az}^2)^2}\left[r^2 \frac{d}{dr}\left(\frac{V_{A\phi}^2 - V^2}{r^2}\right)(\omega^2 - k^2 V_{Az}^2) - \frac{4}{r}(kV_{A\phi}V_{Az} - \omega V)^2\right] u \tag{3.21}$$

According to Knobloch (1992) and Julien & Knobloch (2010), the exponentially growing mode $\omega = -i\lambda$, $\lambda > 0$ is possilbe when the eigenvalue relation has following form

$$(\lambda^2 + k^2 V_{Az}^2)^2 = \frac{k^2}{D}\int_{r_1}^{r_2}\left[r^2 \frac{d}{dr}\left(\frac{V_{A\phi}^2 - V^2}{r^2}\right)(\lambda^2 + k^2 V_{Az}^2) + \frac{4}{r}(kV_{A\phi}V_{Az} - i\lambda V)^2\right]|u|^2 dr. \tag{3.22}$$

Considering the imaginary part of the equation, we have

$$\int_{r_1}^{r_2} \frac{1}{r} V_\phi V |u|^2 dr = 0 \tag{3.23}$$

Knobloch (1992) showed that exponentially growing instability is only possible when $V_{A\phi}$ or V changes sign somewhere in $r_1 < r < r_2$.

4. Laboratory Experiments

Experiments: Donnelly and Ozima 1960 = use magnetic fields to stabilize centrifugal instability of Taylor-Couette flow; Ji et al. 2001 and others = use magnetic fields to generate instability in otherwise stable Taylor-Couette flow

Three types of MRI experiments: 1) standard MRI = axial magnetic field, 2) helical MRI = axial and azimuthal magnetic fields, 3) azimuthal MRI = only azimuthal magnetic fields

4.1. *Standard MRI*

Axial magnetic field

Ji *et al.* (2001), Goodman & Ji (2002) = first modern MRI experiments

Sisan *et al.* (2004) = inner rotating (copper) sphere, outer fixed (steel) sphere, liquid sodium; found β_c above which MRI occurred.

Obstacles of standard MRI in lab experiments: keeping background flow laminar (to ensure that the first instability was MRI and not turbulence); minimize Ekman effect; achieve high enough speeds without breaking experiment

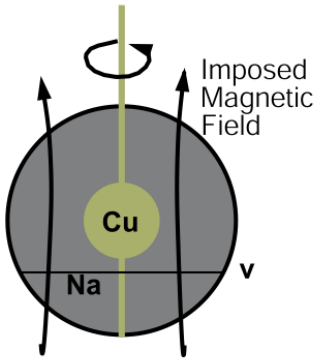

[t]

FIGURE 2. Diagram from Sisan *et al.* (2004) showing the experimental setup. The fixed outer steel sphere contains liquid sodium (the conducting fluid), with the magnetic field imposed coaxially to the rotating inner copper sphere. The magnetic fields and fluid velocity are measured using Hall probes and Doppler velocimetry.

4.2. *Helical MRI*

Hollerbach & Rudiger (2005) = proposed helical (axial + azimuthal magnetic fields) to allow MRI at lower Reynolds

Stefani *et al.* (2006, 2007) = experimentally proved helical MRI

Stefani *et al.* (2009) = improve helical MRI experiment

4.3. *Azimuthal MRI*

Azimuthal magnetic fields only (no axial)

5. Numerical Work

MRI: occurs in a Rayleigh-Stable regime whenever a weak poloidal magnetic field is present.

Accretion can only occur with a efficient mechanism for outward transport of angular momentum. There are many suggested processes that can lead to efficient accretion but none leads to substantial outward angular momentum transport. Before using any model, there is a need to understand the angular momentum transport characteristics so that the appropriate equations can be used. The flow could be turbulent but there is no clear reason why there would be turbulence since there is no known instability that will encourage turbulent flow.

Numerical simulations are employed to try to explain the anomalous viscosity and magnetic field generation. Viscous stresses is insufficient for explaining the outward transport of angular momentum so there is a need for some other mechanism. Purely hydrodynamic flow will not generate that as will be shown by HGB and a weak magnetic field is needed. A strong magnetic field will suppress MRI as shown by Liu (2008). From linear stability analysis of the exact nonlinear streaming solution done by Goodman (1994), we know the magnetic field perturbations grows exponentially, indicating that the solution is unstable. 3D numerical simulation will help to confirm this analysis.

Direct numerical simulations (DNS) are done to solve the magnetohydrodynamic equations for: compressible and incompressible; ideal and non-ideal; 2D and 3D; axisymmetric and non-axisymmetric; field strength; resolution; computational domain size; incorporation of coriolis; and tidal forcing.

With regards to 2D vs 3D simulations, a good comparison was done by Hawley (1995) HGB where they did a local shearing box model which incorporated coriolis and tidal forcing but neglects background gradients in pressure and density (not important unless radial oscillations are significant). Periodic boundary conditions were used with an added shearing component to the radial direction. " Method of characteristics-constrained transport" algorithm as explained in Hawley (1995) was implemented.

The comparison of the 3D simulations results from HGB with the 2D results from Balbus et al BGH 1994 shows significant difference. The 2D results have a general channel/streaming flow solution whereas the 3D results may go through the channel flow but eventually evolves further into a turbulent flow with some not going through the channel flow at all. Note: vertical component of gravity, hence buoyancy, was ignored and since their simulations showed significant density contrast, the shearing box model is not self-consistent. Purely hydrodynamic turbulence did not give significant angular momentum transport needed even when the initial conditions had strong turbulence structures. Their 3D results suggest that accretion disks are well described by Euler's, ignoring the viscous terms from Navier Stokes.

Squire's theorem says that for each unstable 3D disturbances, there are corresponding 2D disturbance that are more unstable. How does that apply here?

Non-axisymmetric Fleming (2000) - suggest saturation does occur even when Elsasser numb $\Delta \geq 1$ if non-axisymmetric disturbances are allowed to evolve.

If Alfven speed is slower than sound speed, equations can be simplified to be incompressible since it is not fundamental to the instability Balbus & Hawley (1991) ...

Incompressible shearing box : Lesur (2007)

Liu (2008) (also Princeton MRI experiments) simulated nonlinear development of MRI in a non-ideal magnetohydrodynamic Taylor-Couette flow (mimicking an on-going experiment) using ZEUS-MP 2.0 code (Hayes (2006)), which is a time-explicit, compressible, astrophysical ideal MHD parallel 3D code with added viscosity and resistivity for axisymmetric flows in cylindrical coordinates. He shows that the saturation of MRI causes a inflowing 'jet' feature which is opposite to the usual Ekman circulation and enhances angular momentum transport radially outward, which is what is needed, agreeing with HGB. Note: Stable MRI regime ($Re \leq 1600$) enhances vertical angular momentum transport while in unstable MRI regime ($Re \geq 3200$), MRI kicks in, resulting in more radial angular momentum transport as compared with vertical.

The use of the shearing box model has its limitations as pointed out by HGB as they do not permit any dynamics involving the background shear, which is taken as imposed and constant in space and time. Regev (2008).. With regards to resolution which is tied in with the model used, the efficiency of angular momentum transport appears to decrease with improved resolution as shown by Fomang (2007), suggesting that transport rates estimated on basis of ideal MHD are affected by grid-scale dissipation and overestimate the efficiency of angular momentum extraction by MRI. Kapyla (2008) also worked on resolution dependence of α, the Shakura-Sunyaev number and the possible decline of the angular momentum transport rate with decreasing Pm.

Sawai et al 2013 Sawaii (2013) simulated a global 3D MRI axisymmetric, ideal model. They did not find any channel flow solutions as HGB did. Increasing spatial resolution contributed to approximate convergence in the exponential growth rate but not that of the saturation of magnetic field due to large numerical diffusion.

Kirillov *et al.* (2012) presents a unifying description of the helical and azimuthal versions of MRI, and they also identify the universal character of the 'Liu' limit $2(1-2) \approx -0.8284$ for the critical Rossby number. (From this universal characteristics, they are led to the prediction that the

instability will be governed by a mode with an azimuthal wavenumber that is proportional to the ratio of axial to azimuthal applied magnetic field, when this ratio becomes large and the Rossby number is close to the Liu limit)

Miller (1999) worked on vertically stratified disks using a shearing box model and found that turbulent magnetised disk can produce a magnetised corona in laminar flow through MRI.

The influence of viscosity and electrical resistivity on the MRI (see Pessah 2008)

From Julien & Knobloch (2010): Reduced equations- Case A ($\delta = \epsilon, \Lambda = O(1)$)

a) Single Mode theory
b) Stress-free boundary conditions
c) Random initial conditions

Reduced equations- Case B ($\epsilon = O(\delta), \Lambda \gg 1$)

a) Single Mode Solutions
b) Multi-mode Sollutions
c) Random initial Perturbations
d) Dissipation and Saturation

Note: Accretional ejection instability (AEI), as suggested by Caunt (2011), gives the same angular momentum transport needed as compared to the global MRI but the instability requires a fairly strong magnetic field. So need an external source, possibly from MRI.

6. Conclusion

Concluding remarks

REFERENCES

Acheson, D. J. 1972 On the hydromagnetic stability of a rotating fluid annulus. *Journal of Fluid Mechanics* **52**, 529–541.

Acheson, D. J. 1973 Hydromagnetic wavelike instabilities in a rapidly rotating stratified fluid. *Journal of Fluid Mechanics* **61**, 609–624.

Acheson, D J & Hide, R 1973 Hydromagnetics of rotating fluids. *Reports on Progress in Physics* **36** (2), 159.

Balbus, S. A. 2003 Enhanced angular momentum transport in accretion disks. *Ann. Rev. Astron. Astrophys* **41**, 555–597.

Balbus, S. A. 2009 Magnetohydrodynamics of protostellar disks. *ArXiv e-prints* .

Balbus, S. A. & Hawley, J. F. 1991 A powerful local shear instability in weakly magnetized disks. i - linear analysis. ii - nonlinear evolution. *Astrophysical Journal* **376**, 214–233.

Balbus, Steven A. & Hawley, John F. 1998 Instability, turbulence, and enhanced transport in accretion disks. *Rev. Mod. Phys.* **70**, 1–53.

Caunt 2011 .

Chandrasekhar, S. 1960 The stability of non-dissipative couette flow in hydromagnetics. *Proceedings of the National Academy of Science* **46**, 253–257.

Charru, François & de Forcrand-Millard, Patricia 2011 *Hydrodynamic instabilities*, , vol. 37. Cambridge University Press.

Davidson, Peter Alan 2001 *An introduction to magnetohydrodynamics*, , vol. 25. Cambridge university press.

Fleming 2000 .

Fomang 2007 .

Freidberg, Jeffrey P 1987 *Ideal magnetohydrodynamics*. Plenum Press, New York, NY.

Goodman 1994 .

Goodman, J & Ji, HT 2002 Magnetorotational instability of dissipative Couette flow. *Journal of Fluid Mechanics* **462**, 365–382.

Hawley 1995 .

Hayes 2006 .

Hollerbach, Rainer & Rudiger, Gunther 2005 New type of magnetorotational instability in cylindrical taylor-couette flow. *Physical Review Letters* **95**.

Ji, HT, Goodman, J & Kageyama, A 2001 Magnetorotational instability in a rotating liquid metal annulus. *Monthly Notices of the Royal Astronomical Society* **325** (2), L1–L5.

Julien, K. & Knobloch, E. 2010 Magnetorotational instability: recent developments. *Philosophical Transactions of the Royal Society A* **368**, 1607–1633.

Kapyla 2008 .

Kirillov, Oleg N., Stefani, Frank & Fukumoto, Yasuhide 2012 A unifying picture of helical and azimuthal magnetorotational instability, and the universal significance of the liu limit. *The Astrophysical Journal* **756** (1), 83.

Knobloch, E. 1992 On the stability of magnetized accretion discs. *Monthly Notices of the Royal Astronomical Society* **255**, 25P–28P.

Lesur 2007 .

Liu, Wei 2008 Numerical study of the magnetorotational instability in princeton mri experiment. *The Astrophysical Journal* **684** (1), 515.

Miller 1999 .

Pessah 2008 .

Regev 2008 .

Sawaii 2013 .

Sisan, Daniel R., Mujica, Nicolás, Tillotson, W. Andrew, Huang, Yi-Min, Dorland, William, Hassam, Adil B., Antonsen, Thomas M. & Lathrop, Daniel P. 2004 Experimental observation and characterization of the magnetorotational instability. *Phys. Rev. Lett.* **93**, 114502.

Stefani, Frank, Gerbeth, Gunter, Gundrum, Thomas, Hollerbach, Rainer, Priede, J ānis, Rüdiger, Günther & Szklarski, Jacek 2009 Helical magnetorotational instability in a taylor-couette flow with strongly reduced ekman pumping. *Phys. Rev. E* **80**.

Stefani, Frank, Gundrum, Thomas, Gerbeth, Gunter, Rüdiger, Günther, Schultz, Manfred, Szklarski, Jacek & Hollerbach, Rainer 2006 Experimental evidence for magnetorotational instability in a taylor-couette flow under the influence of a helical magnetic field. *Phys. Rev. Lett.* **97**.

Stefani, Frank, Gundrum, Thomas, Gerbeth, Gunter, Rdiger, Gnther, Szklarski, Jacek & Hollerbach, Rainer 2007 Experiments on the magnetorotational instability in helical magnetic fields. *New Journal of Physics* **9** (8).

Wikipedia 2013 Magnetorotational instability — Wikipedia, the free encyclopedia. [Online; accessed 29-May-2013].